

Volatile Donor-Functionalized Alkoxy Derivatives of Lutetium and Their Structural Characterization¹

Reiner Anwander,^{*,†} Florian C. Munck,[‡] Thomas Priermeier,[‡] Wolfgang Scherer,[‡] Oliver Runte,[‡] and Wolfgang A. Herrmann[‡]

Institut für Technische Chemie I, Universität Stuttgart, Pfaffenwaldring 55, D-70569 Stuttgart, Germany, and Anorganisch-chemisches Institut, Technische Universität München, Lichtenbergstrasse 4, D-85747 Garching, Germany

Received January 8, 1997[⊗]

Reaction of β -functionalized alcohols of type $\text{HOCR}_2\text{CH}_2\text{do}$ (**1a**, do = OMe, R = Me; **1b**, do = OMe, R = Et; **1c**, do = NMe₂, R = Me) with $\text{Ln}[\text{N}(\text{SiMe}_3)_3]_3$ yields highly volatile (sublimation < 100 °C/10⁻³ Torr) and *n*-hexane-soluble homoleptic alkoxide complexes $[\text{Ln}(\text{OCR}_2\text{CH}_2\text{do})_3]$ (**2a–d**, Ln = Y, Lu). A single-crystal X-ray diffraction study of $\text{Lu}(\text{OCMe}_2\text{CH}_2\text{OME})_3$ (**2a**) revealed a dinuclear complex with significantly polarized metal centers originating from asymmetrical ligand association (triple-bridging). Unintentional employment of “metal-contaminated” alcohol **1a** resulted in the formation of *n*-hexane-soluble **3** exhibiting a substantially increased sublimation temperature (>220 °C/10⁻³ Torr). Crystallization of **3** affords single crystals **3a** featuring the tetranuclear constitution $\text{Lu}_4(\text{O})(\text{OH})(\text{OCMe}_2\text{CH}_2\text{OME})_9$. **3a** represents an unprecedented lanthanide alkoxide comprising both oxo and hydroxo units in addition to alkoxide ligands. The Lu_4O_{15} -core structure of **3a** adopts a “butterfly” rather than a tetrahedral geometry. Potentially tridentate alcohols $\text{HOC}i\text{Bu}(\text{CH}_2\text{O}i\text{Pr})_2$ (**4**) and $\text{HOC}i\text{Pr}_2\text{CH}_2\text{OCH}_2\text{OME}$ (**5**) afford alkoxide complexes “ $\text{Nd}(\text{OR})_3$ ” (**6**, **7**) of reduced volatility. **2a** crystallizes from *n*-hexane at ambient temperature in space group $P2_1/n$ with $a = 13.510(1)$ Å, $b = 15.130(1)$ Å, $c = 38.953(4)$ Å, $\beta = 93.11(1)^\circ$, $V = 7950$ Å³, and $Z = 8$. Least-squares refinement of the model based on 11 747 reflections ($I > 2.0 \sigma(I)$) converged to a final $R = 3.5\%$. **3a** crystallizes from *n*-hexane at -35 °C in space group Cc with $a = 21.63(1)$ Å, $b = 14.49(3)$ Å, $c = 21.04(2)$ Å, $\beta = 109.70(3)^\circ$, $V = 6209$ Å³, and $Z = 4$. Least-squares refinement of the model based on 6057 reflections ($I > 3.0 \sigma(I)$) converged to a final $R = 6.7\%$.

Introduction

Current interest in the chemistry of yttrium and lanthanide alkoxides, preferably monolanthanide derivatives, is mainly due to their potential as precursors in *CVD*^{2,3} and *sol–gel* technology^{4,5} and as catalysts in selective organic transformations.⁶ The type of alkoxide ligand markedly affects crucial properties such as mononuclearity, volatility, solubility, basicity, and stability against hydrolysis. For example, donor-functionalized alcohols proved to be superior to conventional alcohols such as $\text{HO}i\text{Pr}$ or $\text{HO}i\text{Bu}$ with respect to their application in the *sol–gel* process.^{4,5} We⁷ and others^{8–15} are currently investigating alkoxide systems exhibiting the components Ln

and donor-functionalized alcohols. We found that donor-functionalized alkoxides of type $\text{Ln}(\text{OCR}^1_2\text{CH}_2\text{OR}^2)_3$ containing a sterically demanding group in the α -position ($\text{R}^1 = i\text{Bu}$, $i\text{Pr}$) are highly soluble and volatile.⁷ Due to the pronounced solubility of these alkoxide complexes even in nonpolar solvents we were not able to prove their mononuclear composition by X-ray structure analysis. Fortunately, other donor-functionalized alcohols have been designed which compromise the crystallization behavior. Both the accommodation of higher homologous elements, as evidenced by the molecular structures of $\text{Ln}(\text{OC}i\text{Bu}_2\text{CH}_2\text{PMe}_2)_3$ ⁹ and related siloxide complexes,¹⁴ and the attachment of more rigid donor groups such as methylpy-

[†] Universität Stuttgart.

[‡] Technische Universität München.

[⊗] Abstract published in *Advance ACS Abstracts*, July 1, 1997.

- (1) Part 7: Herrmann, W. A.; Anwander, R.; Dufaud, V.; Scherer, W. *Angew. Chem., Int. Ed. Engl.* **1994**, *33*, 1285.
- (2) (a) Bradley, D. C. *Chem. Rev.* **1989**, *89*, 1317. (b) Bradley, D. C. *Polyhedron* **1994**, *13*, 1111.
- (3) Herrmann, W. A.; Huber, N. W.; Runte, O. *Angew. Chem., Int. Ed. Engl.* **1995**, *34*, 2187.
- (4) (a) Hubert-Pfalzgraf, L. G. *New J. Chem.* **1995**, *19*, 727. (b) Hubert-Pfalzgraf, L. G. *New J. Chem.* **1987**, 663. (c) Hubert-Pfalzgraf, L. G. *Appl. Organomet. Chem.* **1992**, *6*, 627. (d) Sanchez, C.; Livage, J. *New J. Chem.* **1990**, *14*, 513.
- (5) (a) Monde, T.; Kosuka, H.; Sakka, S. *Chem. Lett.* **1988**, 287. (b) Goel, S. C.; Kramer, K. S.; Gibbons, P. C.; Buhro, W. E. *Inorg. Chem.* **1989**, *28*, 3620. (c) Rupich, M. W.; Lagos, B.; Hachey, J. P. *Appl. Phys. Lett.* **1989**, *55*, 2447. (d) Katayama, S.; Sekine, M. *J. Mater. Res.* **1990**, *5*, 683. (e) Hampson, P. J.; Leedham, T. J. *Chemtronics* **1991**, *5*, 115. (f) Antonelli, D. M.; Nakahira, A.; Ying, J. Y. *Inorg. Chem.* **1996**, *35*, 3126. (g) Abdel-Fattah, T. M.; Pinnavaia, T. J. *Chem. Commun.* **1996**, 665.
- (6) Anwander, R. *Top. Curr. Chem.* **1996**, *179*, 149.
- (7) Herrmann, W. A.; Anwander, R.; Denk, M. *Chem. Ber.* **1992**, *125*, 2399.

- (8) Buhro's work on highly volatile d-transition metal alkoxides based on commercially available β -functionalized alcohols was path breaking: Goel, S. C.; Kramer, K. S.; Chiang, M. Y.; Buhro, W. E. *Polyhedron* **1989**, *9*, 611.
- (9) Hitchcock, P. B.; Lappert, M. F.; MacKinnon, I. A. *J. Chem. Soc., Chem. Commun.* **1988**, 1557.
- (10) Gradeff, P. S.; Mauermann, H.; Schreiber, F. G. *J. Less-Common Met.* **1989**, *149*, 87.
- (11) (a) Poncelet, O.; Hubert-Pfalzgraf, L. G.; Daran, J.-C.; Astier, R. *J. Chem. Soc., Chem. Commun.* **1989**, 1846. (b) Poncelet, O.; Hubert-Pfalzgraf, L. G.; Daran, J.-C. *Inorg. Chem.* **1990**, *29*, 2883. (c) Sirio, C.; Poncelet, O.; Hubert-Pfalzgraf, L. D.; Daran, J. C.; Vaissermann, J. *Polyhedron* **1992**, *11*, 177. (d) Hubert-Pfalzgraf, L. G.; Khokh, N. E.; Daran, J.-C. *Polyhedron* **1992**, *11*, 59.
- (12) McLain, S. J.; Drysdale, N. E. U.S. Patent 5,028,667, 1991. (b) McLain, S. J.; Ford, T. M.; Drysdale, N. E. *Am. Chem. Soc. Div. Polym. Chem.* **1992**, *33*, 463.
- (13) Hogerheide, M. P.; Ringelberg, S. N.; Grove, D. M.; Jastrzebski, J. T. B. H.; Boersma, J.; Smeets, W. J. J.; Spek, A. L.; van Koten, G. *Inorg. Chem.* **1996**, *35*, 1185.
- (14) (a) Shao, P.; Berg, D. J.; Bushnell, G. W. *Inorg. Chem.* **1994**, *33*, 3452. (b) Shao, P.; Berg, D. J.; Bushnell, G. W. *Inorg. Chem.* **1994**, *33*, 6334.
- (15) Evans, W. J.; Anwander, R.; Berlekamp, U. H.; Ziller, J. W. *Inorg. Chem.* **1995**, *34*, 3583.

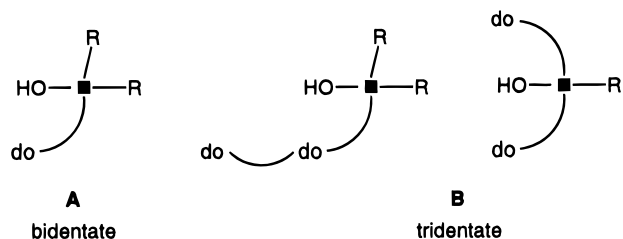


Figure 1. ■ = C_α atom (center of branching) and do = donor functionality, e.g., OR, NR₂.

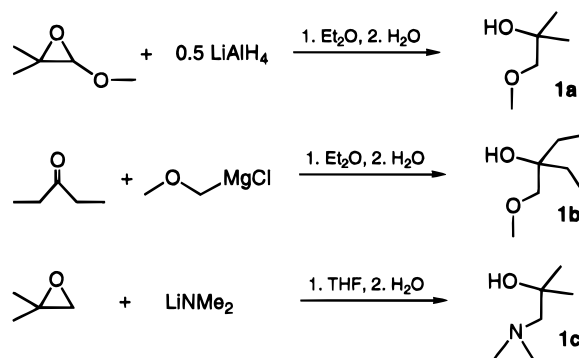
ridine ensure mononuclearity,¹⁵ however, by the loss of volatility. By way of contrast, reducing the steric bulk in the α-position also decreases solubility and hence supports crystallization. Representative, structurally characterized derivatives include the cyclic decamer [Y(OCH₂CH₂OMe)₃]₁₀^{11a} and the heteroleptic Ce(IV) complex Ce₂(O*i*Pr)₆(OC₂H₄NMeC₂H₄NMe₂)₂.^{11d} Following our studies on well-crystallizing, homoleptic, volatile, and mononuclear donor-functionalized alkoxide complexes derived from HOCMe₂CH₂OMe (**1a**) and M = Cr and Bi,¹⁶ we anticipated further attempts to direct the habit of donor-functionalized alkoxides of the rare earth elements by both the variation of (i) the steric bulk in the α-position and (ii) the type and number of donor functionalities. Our concept of ligand design as outlined in Figure 1 includes the bidentate A-type as a promising ligand for stabilizing Ln(III) and Ce(IV) species, while tridentate B- and C-type alcohols were originally designed to stabilize Ln(II) complexes.¹⁷ In addition, we can present the effect of serendipitous amounts of water on the nuclearity of such a donor-functionalized alkoxide.

Results and Discussion

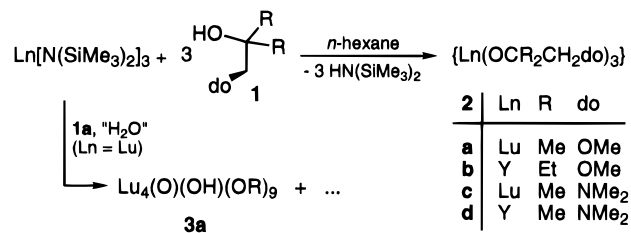
Derivatives of Bidentate Alcohols HOCMe₂CH₂OMe (1a), HOCe₂CH₂OMe (1b), and HOCMe₂CH₂NMe₂ (1c). The employed donor-functionalized alcohols were synthesized according to standard organic procedures as summarized in Scheme 1.^{18–20} Typically, the reduced CH bulk renders these alcohols highly polarized and hydrophilic. Therefore, care has to be taken during the workup procedures of the crude reaction products. The alcohols form azeotropic mixtures with water during the final distillation and, hence, when used without further precaution, lead to the formation of partially hydrolyzed alkoxide clusters (*vide infra*). Quenching of the reaction mixture with a stoichiometric amount of water and subsequent drying of the distilled alcohols over molecular sieves (3 Å) for several days proved to be quite efficient in providing dry alcohols.

All alkoxide complexes were synthesized according to the silylamide route at ambient temperature (Scheme 2).²¹ In order to suppress oligomerization as much as possible, we selected

Scheme 1



Scheme 2



the lanthanide elements yttrium and lutetium for the reason of the smaller ionic radius.²² Reaction of the silylamide complexes with 3 equiv of donor-functionalized alcohols **1** in *n*-hexane afforded clear solutions. The resulting alkoxide complexes **2** were isolated as white powders and in the case of the amino-functionalized systems as colorless oily residues, respectively, and characterized by means of IR and NMR spectroscopy, mass spectrometry, elemental analysis, and the sublimation behavior. IR spectroscopy proved to be a valuable and quick tool to check the completeness of the reactions. The CI mass spectrometric studies all gave the dinuclear species as the parent molecular ion. The species [Ln₂(OR)₅]⁺ occurred as the fragment ion with the highest intensity. Room-temperature NMR spectra (¹H, ¹³C) displayed one type of alkoxide ligand in each complex. A variable ¹H NMR study of **2a** in toluene-*d*₈ revealed that the OMe protons remain equivalent in the temperature range –80 to 20 °C. However, the signal for the methyl protons of the C_α atom (δ = 1.57 ppm) broadens at –30 °C and two methyl resonances occur in a 2:1 ratio on further cooling to –40 °C (δ = 1.54 and 1.36 ppm). At –50 °C, the signal at δ = 1.54 ppm splits up into two separate signals of equal intensity. The three signals coalesce again on further cooling to –60 °C and become extremely broad at –70 °C. Similar observations are made for the C_β-ethylene protons; however, the signals appear less resolved and broader. Such a distinct NMR behavior has to be ascribed to the presence of different coordination modes of the ligands usually evolving from exchange processes such as “terminal/bridging” ligand redistribution or “arm on–arm off” processes of the donor functionalities.¹⁴ We conducted an X-ray analysis of **2a** to further substantiate a dinuclear molecular arrangement and the presence of coordinatively different alkoxide ligands.

Solid-State Structure of 2a. Single crystals of **2a** were grown by slow evaporation of *n*-hexane from a saturated solution at ambient temperature. The summary of data collection and crystallographic parameters and selected bond lengths and angles are collected in Tables 1 and 4. The X-ray structure analysis reveals the presence of two independently crystallizing dinuclear

- (16) Herrmann, W. A.; Huber, N. W.; Anwander, R.; Priermeier, T. *Chem. Ber.* **1993**, *126*, 1127.
 (17) Anwander, R. Ph.D. Thesis, **1992**, Technical University, Munich, 1992.
 (18) Brown, H. C.; Yoon, N. M. *J. Am. Chem. Soc.* **1966**, *88*, 1464.
 (19) (a) Palomaa, M. H. *Ber. Dtsch. Chem. Ges.* **1909**, *42*, 3873. (b) Palomaa, M. H. *Chem. Zentralbl.* **1918**, *89*, 1144. (c) Taeger, E.; Kahlert, E.; Walter, H. *J. Prakt. Chem.* **1965**, *28*, 13. (d) Normant, N.; Crisan, C. *Bull. Soc. Chim.* **1959**, 459. (e) Castro, B. *Bull. Soc. Chim.* **1967**, 1533. (f) Wilson, K. W.; Roberts, J. D.; Young, W. G. *J. Am. Chem. Soc.* **1950**, *72*, 218. (g) Benkeser, R. A.; Young, W. G.; Broxterman, W. E.; Jones, D. A., Jr.; Piaseczynski, S. *J. Am. Chem. Soc.* **1969**, *91*, 132.
 (20) (a) McManus, S. P.; Larso, C. A.; Hearn, R. A. *Synth. Commun.* **1973**, *3*, 177. (b) Chini, M.; Crotti, P.; Macchia F. *Tetrahedron Lett.* **1990**, *31*, 4661. (c) Nugent, W. A.; Harlow, R. L. *J. Am. Chem. Soc.* **1994**, *116*, 6142.
 (21) (a) Hitchcock, P. B.; Lappert, M. F.; Singh, A. *J. Chem. Soc., Chem. Commun.* **1983**, 1499. (b) Anwander, R. *Top. Curr. Chem.* **1996**, *179*, 33.

- (22) Shannon, R. D. *Acta Crystallogr.* **1976**, *A32*, 751.
 (23) Sandstrom, J. *Dynamic NMR Spectroscopy*; Pergamon: London, 1982; pp 77–91.

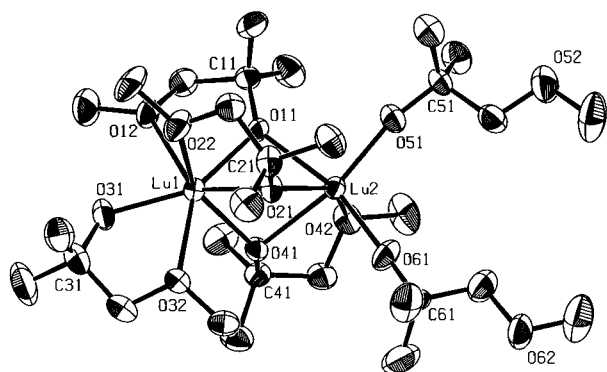


Figure 2. Molecular structure of $\text{Lu}_2(\mu_2, \eta^2\text{-OR})(\eta^2\text{-OR})(\eta^1\text{-OR})_2$ (**2a**) (PLATON^{53a} plot). Thermal ellipsoids are drawn at the 50% probability level.

Table 1. Selected Bond Distances (Å) and Angles (deg) for **2a**

Molecule 1			
Lu(1)–O(11)	2.220(3)	Lu(1)–O(21)	2.232(3)
Lu(1)–O(31)	2.123(3)	Lu(1)–O(41)	2.196(3)
Lu(1)–O(12)	2.424(3)	Lu(1)–O(22)	2.381(4)
Lu(1)–O(32)	2.468(3)	Lu(2)–O(11)	2.308(3)
Lu(2)–O(21)	2.233(3)	Lu(2)–O(41)	2.373(3)
Lu(2)–O(51)	2.058(3)	Lu(2)–O(61)	2.053(3)
Lu(2)–O(42)	2.343(3)	Lu(1)–Lu(2)	3.2229(3)
O(11)–Lu(1)–O(12)	66.5(1)	O(21)–Lu(1)–O(22)	68.9(1)
O(31)–Lu(1)–O(32)	68.5(1)	Lu(1)–O(11)–C(11)	128.9(3)
Lu(1)–O(21)–C(21)	122.7(3)	Lu(1)–O(31)–C(31)	126.6(3)
Lu(1)–O(41)–C(41)	133.4(3)	O(41)–Lu(2)–O(42)	69.2(1)
Lu(2)–O(11)–C(11)	140.4(3)	Lu(2)–O(21)–C(21)	134.4(3)
Lu(2)–O(41)–C(41)	118.6(3)	Lu(2)–O(51)–C(51)	166.4(3)
Lu(2)–O(61)–C(61)	174.8(4)		
Molecule 2			
Lu(3)–O(71)	2.207(3)	Lu(3)–O(81)	2.242(3)
Lu(3)–O(91)	2.125(3)	Lu(3)–O(101)	2.192(3)
Lu(3)–O(72)	2.435(3)	Lu(3)–O(82)	2.363(3)
Lu(3)–O(92)	2.441(4)	Lu(4)–O(71)	2.303(3)
Lu(4)–O(81)	2.224(3)	Lu(4)–O(101)	2.378(3)
Lu(4)–O(111)	2.057(3)	Lu(4)–O(121)	2.048(3)
Lu(4)–O(102)	2.366(3)	Lu(3)–Lu(4)	3.2249(3)
O(71)–Lu(3)–O(72)	66.3(1)	O(81)–Lu(3)–O(82)	69.0(1)
O(91)–Lu(3)–O(92)	69.2(1)	Lu(3)–O(71)–C(71)	129.1(3)
Lu(3)–O(81)–C(81)	122.7(3)	Lu(3)–O(91)–C(91)	125.5(3)
Lu(3)–O(101)–C(101)	132.8(3)	O(101)–Lu(4)–O(102)	69.1(1)
Lu(4)–O(71)–C(71)	139.4(3)	Lu(4)–O(81)–C(81)	134.3(3)
Lu(4)–O(101)–C(101)	118.4(3)	Lu(4)–O(111)–C(111)	163.0(3)
Lu(4)–O(121)–C(121)	170.1(4)		

molecules. Molecule 1 is shown in Figure 2. Although the formation of dinuclear species is routinely observed in lanthanide alkoxide chemistry,²⁴ the overall molecular arrangement of **2a** comprises an unusual alkoxide ligation. The lutetium centers are asymmetrically bridged by three $\mu_2\text{-}\eta^2$ ligands and therefore experience a completely different alkoxide environment. While the bridging of two lanthanide centers by three $\mu\text{-O}$ (alkoxide) ligands is commonly observed in higher agglomerized complexes such as $[\text{La}(\text{O}i\text{Bu})_3]$,²⁵ there are only a few structurally characterized dinuclear complexes featuring this coordination mode. For example, a previously reported oligosilsesquioxane complex of yttrium exhibits three $\mu\text{-O}$ (siloxide) bridges.¹

Lu1 (Lu3) is 7-coordinated by four O(alkoxide) and three O(ether) atoms. One terminal η^2 -alkoxide ligand (bite angle,

68.5(1), 69.2(1)°) and two ether functionalities of the three bridging alkoxide ligands define the coordination environment. Two bridging alkoxide ligands bearing the coordinating ether groups are located closer to Lu1 (Lu3) to compensate a formal charge deficiency. Despite 6-coordination, Lu2 (Lu4) is formally exposed to a higher negative charge arising from five coordinating alkoxide ligands (two terminal and three bridging). An ether group of one bridging ligand completes the distorted trigonal prismatic coordination geometry at Lu2 (Lu4).

The terminal η^1 -alkoxide ligands at Lu2 (O51; O61) and Lu4 (O111; O121) show bond lengths in the range 2.048(3)–2.058(3) Å. The terminal Lu–O(alkoxide) bond distances of 2.123(3) and 2.125(3) Å at Lu1 (O31) and Lu3 (O91), respectively, are comparatively elongated due to the higher coordination number of the metals and probably ring strain. This is further documented by the longest Lu–O(ether, O32, O92) distances of 2.468(3) Å within these chelating moieties. The terminal Lu–O bond distances correlate well with the Lu–O(phenoxide) distances of 2.048(7)–2.066(6) Å detected in 8-coordinated, 1,3-bis(diethylamide)-substituted calix[4]arene complexes of type $[\text{Lu}(\text{L-2H})(\text{picrate})]$ (L = 5,11,17,23-tetra-*tert*-butyl-25,27-bis((diethylcarbamoyl)methoxy)-26,28-dihydroxycalix[4]-arene).²⁶ The bridging Lu–O bond distances of **2a** range from 2.192(3) to 2.378(3) Å, reflecting the asymmetry of this molecular fragment. For comparison, the complex $\{\text{ClLu}[\text{OC}_6\text{H}_2(\text{CH}_2\text{NMe}_2)_2\text{-2,6-Me-4}]_3\text{Na}\}$ exhibits a 7-coordinate lutetium center with bridging Lu–O distances of 2.143(3)–2.174(3) Å.¹³ The other Lu–O(ether) contacts range from 2.343(3) to 2.435(3) Å and are therefore comparable to the Lu–O(THF) bond lengths in $\text{Cp}_2\text{Lu}(\text{NC}_4\text{H}_2\text{Me}_2)(\text{THF})$ (2.302(3) Å)²⁷ and $\text{Cp}_3\text{Lu}(\text{THF})$ (2.39(2) Å).²⁸ One of the three $\mu_2\text{-}\eta^2$ -bridging ligands shows equal Lu–O(alkoxide) bond lengths (Lu–O21, 2.232(3), 2.333(3) Å; Lu–O81, 2.242(3), 2.224(3) Å), and the coordinated ether groups Lu1–O22 (2.381(3) Å) and Lu3–O82 (2.363(3) Å) accomplish bite angles of 68.9(1) and 69.0(1)°, respectively. The two O(alkoxide) atoms O11, O41 (O71, O101) of the other $\mu_2\text{-}\eta^2$ -bridging ligands which are significantly closer to Lu1 (Lu3) (Lu1/2–O11, 2.220(3), 2.308; Lu1/2–O41, 2.196(3), 2.373(3); Lu3/4–O71, 2.207(3), 2.303(3); Lu3/4–O101, 2.192(3), 2.378(3) Å) form together with the ether donor functionalities (Lu1–O12, 2.424(3); Lu2–O42, 2.343(3); Lu3–O72, 2.435(3); Lu4–O102, 2.366(3) Å) bite angles ranging from 66.3(1) to 69.2(1)°. The Lu–O–C bond angles of the chelating ligands lie in the range 118.4(3)–140.4(3)°. The Lu–O–C bond angles of the terminal alkoxide ligands range from 163.0(3) to 174.8(4)°.

The Effect of Water: Isolation and Structural Characterization of an Oxo–Hydroxo–Alkoxide Cluster. When we were initially aiming at the homoleptic complex $[\text{Lu}(\text{OCMe}_2\text{-CH}_2\text{OMe})_3]$ (**2a**), a quantity of alcohol **1a** was employed which was not predried over molecular sieves. Upon addition of such **1a** to $\text{Lu}[\text{N}(\text{SiMe}_3)_2]_3$ in a 3:1 molar ratio a small amount of white precipitate formed (Scheme 1). Apart from the characteristic ligand vibrations, the IR spectra of this residue showed a broad absorption at $\nu = 3730\text{--}3220\text{ cm}^{-1}$ which is typical of intermolecular bridging of hydroxo groups. Evaporation of the *n*-hexane solution yielded a white powder designated as **3**. Residue **3** is less soluble in *n*-hexane than complexes **2** or donor-functionalized derivatives accommodating sterically more demanding groups in the α -position.⁷ The CI mass spectrum of

(24) (a) Mehrotra, R. C.; Singh, A.; Tripathi, U. M. *Chem. Rev.* **1991**, *91*, 1287. (b) Herrmann, W. A.; Anwender, R.; Scherer, W. *Chem. Ber.* **1993**, *126*, 1533. (c) Barnhart, D. M.; Clark, D. L.; Huffman, J. C.; Vincent, R. L.; Watkin, J. G. *Inorg. Chem.* **1993**, *32*, 4077 and references therein.
(25) Bradley, D. C.; Chudzynska, H.; Hursthouse, M. B.; Motevalli, M. *Polyhedron* **1991**, *10*, 1049.

(26) (a) Beer, P. D.; Drew, M. G. B.; Grieve, A.; Kan, M.; Leeson, P. B.; Nicholson, G.; Ogden, M. I.; Williams, G. *Chem. Commun.* **1996**, 1117. (b) Beer, P. D.; Drew, M. G. B.; Kan, M.; Leeson, P. B.; Ogden, M. I.; Williams, G. *Inorg. Chem.* **1996**, *35*, 2202.
(27) Schumann, H.; Lee, P. R.; Dietrich, A. *Chem. Ber.* **1990**, *123*, 1331.
(28) Ni, C.; Deng, D.; Qian, C. *Inorg. Chim. Acta* **1985**, *110*, L7.

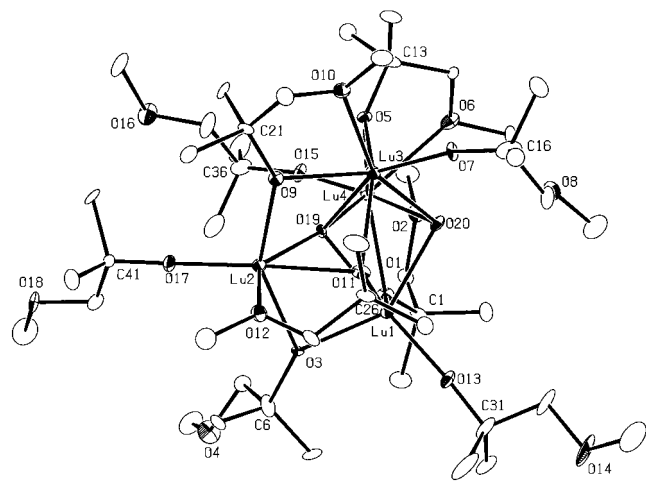


Figure 3. Molecular structure of $\text{Lu}_4(\mu_4\text{-O})(\mu_3\text{-OH})(\mu_3,\eta^2\text{-OR})(\mu_2,\eta^2\text{-OR})_3(\mu_2,\eta^1\text{-OR})(\eta^1\text{-OR})_4$ (**3a**) (PLATON^{53a} plot). Thermal ellipsoids are drawn at the 40% probability level.

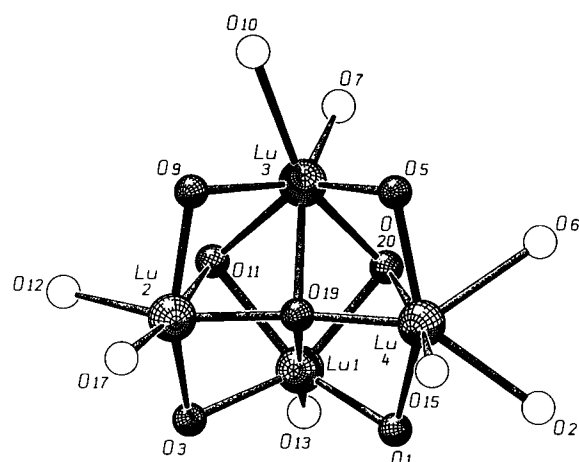


Figure 4. View of the Lu_4O_{15} core of **3a** (SCHAKAL^{53b} plot). The “inner core” structure (shaded) has a local C_3 symmetry.

3 contains the species $[\text{Lu}_2(\text{OR})_5]^+$ as base peak and a series of intense ions, among them the trinuclear fragment ions $[\text{Lu}_3(\text{OR})_9]^+$ and $[\text{Lu}_3(\text{OR})_9(\text{HOR})]^+$, the latter indicating still higher agglomeration. Noteworthy in the IR spectra of **3** is a sharp absorption at $\nu = 3487 \text{ cm}^{-1}$ which is typical of isolated OH functionalities.²⁹ Despite that complete sublimation of material **3** occurs in a narrow temperature range, the very complex ¹H NMR spectrum probably points out the presence of more than one molecular species.

Cooling of an *n*-hexane solution of sublimed **3** to $-35 \text{ }^\circ\text{C}$ afforded a crop of single crystals of **3a** suitable for an X-ray structural characterization. The molecular structure of **3a** features a tetranuclear oxo-hydroxo cluster^{30,31} of net composition $\text{Lu}_4\text{O}(\text{OH})(\text{OR})_9$ (Figures 3 and 4). Important bond distances and angles are summarized in Table 2. The central Lu_4 unit adopts a “butterfly” arrangement rather than a tetrahedral geometry.³² There are two longer distances (Lu1-Lu3 , 3.423(2); Lu2-Lu4 , 4.211(2) Å) and four distances in the

Table 2. Selected Bond Distances (Å) and Angles (deg) for **3a**

Lu(1)-O(13)	2.04(2)	Lu(2)-O(17)	2.06(2)
Lu(3)-O(7)	2.04(2)	Lu(4)-O(15)	2.08(2)
Lu(1)-O(11)	2.35(2)	Lu(2)-O(11)	2.47(3)
Lu(3)-O(11)	2.35(2)	Lu(1)-O(1)	2.18(2)
Lu(4)-O(1)	2.31(2)	Lu(3)-O(5)	2.14(2)
Lu(4)-O(5)	2.30(2)	Lu(2)-O(9)	2.19(2)
Lu(3)-O(9)	2.29(2)	Lu(1)-O(3)	2.22(2)
Lu(2)-O(3)	2.22(2)	Lu(2)-O(12)	2.31(2)
Lu(1)-O(10)	2.53(2)	Lu(4)-O(2)	2.44(2)
Lu(4)-O(6)	2.47(3)	Lu(1)-O(19)	2.35(2)
Lu(2)-O(19)	2.10(2)	Lu(3)-O(19)	2.38(2)
Lu(4)-O(19)	2.13(2)	Lu(1)-O(20)	2.27(2)
Lu(3)-O(20)	2.31(2)	Lu(4)-O(20)	2.52(2)
Lu(1)-Lu(2)	3.253(2)	Lu(1)-Lu(3)	3.423(2)
Lu(1)-Lu(4)	3.285(2)	Lu(2)-Lu(3)	3.295(2)
Lu(2)-Lu(4)	4.211(2)	Lu(3)-Lu(4)	3.310(2)
O(1)-Lu(4)-O(2)	69.5(7)	O(5)-Lu(4)-O(6)	69.2(7)
O(9)-Lu(3)-O(10)	65.4(7)	O(11)-Lu(2)-O(12)	68.3(8)
Lu(1)-O(19)-Lu(2)	93.8(7)	Lu(1)-O(19)-Lu(3)	92.8(6)
Lu(1)-O(19)-Lu(4)	94.4(7)	Lu(2)-O(19)-Lu(3)	94.5(8)
Lu(2)-O(19)-Lu(4)	168(1)	Lu(3)-O(19)-Lu(4)	94.5(6)
Lu(1)-O(20)-Lu(3)	96.6(7)	Lu(1)-O(20)-Lu(4)	86.4(7)
Lu(3)-O(20)-Lu(4)	86.4(6)	Lu(3)-O(7)-C(16)	165(2)
Lu(1)-O(13)-C(31)	175(3)	Lu(3)-O(15)-C(36)	155(3)
Lu(2)-O(17)-C(41)	178(3)	Lu(1)-O(1)-C(1)	137(2)
Lu(4)-O(1)-C(1)	118(2)	Lu(1)-O(3)-C(6)	131(2)
Lu(2)-O(3)-C(6)	130(2)	Lu(3)-O(5)-C(13)	137(2)
Lu(4)-O(5)-C(13)	115(2)	Lu(2)-O(9)-C(21)	140(2)
Lu(3)-O(9)-C(21)	121(2)	Lu(1)-O(11)-C(26)	131(2)
Lu(2)-O(11)-C(26)	117(2)	Lu(3)-O(11)-C(26)	128(2)

range 3.253(2)–3.310(2) Å which compare well with **2a** (3.2229(3) Å). The lutetium atoms Lu1 and Lu2 are coordinated by six oxygen atoms, compared to the 7-fold coordination of Lu3 and Lu4. Figure 4 shows the resulting Lu_4O_{15} “core” structure. Considering the Lu_4 unit and the bridging oxygen atoms O1, O3, O5, O9, O11, O19, and O20 only, an “inner core” structure with local C_3 symmetry results. Oxo-centered butterfly Ln_4 units were reported earlier in $\text{Ce}_4(\mu_4\text{-O})(\mu_3\text{-OiPr})_2(\mu_2\text{-OiPr})_4(\text{OrPr})_7(\text{HOiPr})$ ³³ and $[\text{Y}_4(\mu_3\text{-OrBu})_2(\mu\text{-OrBu})_4(\mu\text{-Cl})_2(\text{OrBu})_4\text{Li}_4(\mu\text{-OrBu})_2]_2$.³⁴ Very recently, hexa- and octanuclear oxo-centered species were isolated comprising the donor-functionalized alkoxide ligand $\text{OC}_2\text{H}_4\text{OMe}$, e.g., $\text{Gd}_6(\mu_4\text{-O})(\mu_3,\eta^2\text{-OR})_4(\mu,\eta^2\text{-OR})_6(\mu_2,\eta^1\text{-OR})_2(\eta^1\text{-OR})_4$ ³⁵ and $\text{Pr}_8(\mu_4\text{-O})_4(\mu_3,\eta^2\text{-OR})_4(\mu,\eta^2\text{-OR})_8(\mu_2,\eta^1\text{-OR})_2(\eta^1\text{-OR})_2(\text{OPMe}_3)_2$.³⁶

Inspection of the ligand sphere reveals enhanced structural flexibility of the alkoxide ligand **1a**. There are *four* different modes of coordination that do not include the η^2 -chelating mode present in homoleptic **2a**. Each lutetium atom has one η^1 -terminal alkoxide ligand (O7/O8; O13/O14; O15/O16; O17/O18) with an average bond distance of 2.05(2) Å. For comparison, the terminal $\text{Ln-O}(\text{alkoxide})$ bond lengths in $\text{Yb}_3\text{O}(\text{OiPr})_{13}$ ³⁶ and $[\text{Y}(\text{OC}_2\text{H}_4\text{OMe})_3]_{10}$ ^{11a} are 2.00 and 2.09(2) Å, respectively. One ligand is *asymmetrically* μ_3,η^2 -bridging (O11/O12; bite angle 68.3(8)°) and displays Lu-O bond lengths of 2.35(2), 2.35(2), and 2.47(3) Å which hardly deviate from its $\text{Lu2-O}(\text{ether})$ contact of 2.31(2) Å. The $\text{Lu-O}(\text{alkoxide})$ bond distances of the three *asymmetrically* μ_2,η^2 -bridging ligands (O1/

(29) Herrmann, W. A.; Anwander, R.; Kleine, M.; Öfele, K.; Riede, J.; Scherer, W. *Chem. Ber.* **1992**, *125*, 2391.

(30) Chandler, C. D.; Roger, C.; Hampden-Smith, M. J. *Chem. Rev.* **1993**, *93*, 1205.

(31) Mehrotra, R. C.; Singh, A. *Chem. Soc. Rev.* **1996**, *1*.

(32) Recently, a square planar metal coordination at $\mu_4\text{-O}^{2-}$ was reported in $\text{Na}_6\{[(\text{C}_6\text{H}_5\text{SiO}_2)_8]_2\text{Ln}_4(\mu_4\text{-O})\}$ (Ln = Nd, Gd): (a) Shchegolikina, O. I.; Pozdniakova, Yu. A.; Lindeman, S. V.; Zhdanov, A. A.; Psaro, R.; Ugo, R.; Gavioli, G.; Battistuzzi, R.; Borsari, M.; Rüffer, T.; Zucchi, C.; Pályi, G. *J. Organomet. Chem.* **1996**, *514*, 29. (b) Zucchi,

C.; Shchegolikina, O. I.; Borsari, M.; Cornia, A.; Gavioli, G.; Fabretti, A. C.; Rentschler, E.; Gatteschi, D.; Ugo, R.; Psaro, R.; Pozdniakova, Yu. A.; Lindeman, S. V.; Zhdanov, A. A.; Pályi, G. *J. Mol. Catal.* **1996**, *107*, 313.

(33) Yunlu, K.; Gräff, P. S.; Edelstein, N.; Kot, W.; Shalimoff, G.; Streib, W. E.; Vaartstra, B. A.; Caulton, K. G. *Inorg. Chem.* **1991**, *30*, 2317.

(34) Evans, W. J.; Sollberger, M. S.; Hanusa, T. P. *J. Am. Chem. Soc.* **1988**, *110*, 1841.

(35) Daniele, S.; Hubert-Pfalzgraf, L. G.; Daran, J.-C. *Polyhedron* **1996**, *15*, 1063.

(36) Bradley, D. C.; Chudzynska, H.; Frigo, D. M.; Hammond, M. E.; Hursthouse, M. B.; Mazid, M. A. *Polyhedron* **1990**, *9*, 719.

O2, O5/O6, O9/O10) are longer at those atoms which are coordinated by an additional, relatively long ether group (average 2.48(3) Å; bite angles 65.4(7)–69.5(7)°). The bridging Lu–O(alkoxide) bond distances range from 2.14(2) to 2.31(2) Å and are shortened by approximately 0.1 Å at the 6-coordinated Lu atoms, except for the Lu3–O5 bond of 2.14(2) Å. The atoms Lu1 and Lu2 are linked by the only *symmetrically* μ_2, η^1 -bridging alkoxide ligand (O3/O4; 2.22(2) Å).

The μ_4 -O(oxo) anion is asymmetrically encapsulated by the metal atoms (Lu–O19: 2.38(2), 2.35(2), 2.13(2), 2.10(2) Å) and approximately bisects the long Lu2–Lu4 contact of 4.211(2) Å to afford the two short Lu–O19 contacts and an almost linear Lu2–O19–Lu4 angle (168(1)°). The lutetium atoms with the longer oxo contacts also form the two shorter bonds to the hydroxo oxygen (2.27(2), 2.31(2) Å). The third hydroxo bond distance Lu4–O20 of 2.52(2) Å is relatively long. For comparison the μ_x -oxo–Ln bond lengths are 2.28–2.33 Å in Yb₅O(OiPr)₁₃,³⁶ 2.40(2)–2.52(2) Å in [Y₄O(OtBu)₁₂Cl₂Li₄]₂,³⁴ and 2.003(3) Å in [Cp₂Lu(THF)](μ -O).³⁷ The Lu–O–C angles of the terminal alkoxide ligands lie in the range 155(3)–178(3)°. Considering the entire ligand coordination sphere, the exact description of **3a** is Lu₄(μ_4 -O)(μ_3 -OH)(μ_3, η^2 -OR)(μ_2, η^2 -OR)₃(μ_2, η^1 -OR)(η^1 -OR)₄.

The tendency to incorporate oxygen from “pure” organic solvents to form oxo-centered cluster compounds is well documented for lanthanide alkoxides.^{31,32} However, alkoxide–oxo clusters with an additional hydroxo ligand have not been previously known for lanthanide complexes. Hence, compound **3a** adds a further mosaic to the transition of molecular alkoxide complexes to oxidic materials. Until now, simple ligation of water in Pr[OC₆H₂(CH₂NMe₂)_{3-2,4,6}]₃(H₂O)₂³⁸ and the combinations “H₂O/OH/alkoxide” in, e.g., Cu₄Ln₂(PyO)₈(PyOH)₄(OH)₄(NO₃)₄(H₂O)₂ (Ln = Gd, Dy)³⁹ and “H₂O/O/alkoxide” in, e.g., [Y₂Cu₈(μ_4 -O)(μ -PyO)₁₂(μ -Cl)(NO₃)₄(H₂O)₂·2H₂O]⁴⁰ with PyOH = 2-hydroxypyridine have been structurally established. Hydroxo functionalities were hitherto found as entrapped ligands in alkoxide complexes of type YNa₈(OtBu)₁₀(OH)⁴¹ and dinuclear compounds, e.g., [O(C₂H₄Cp)₂Lu(μ -N₂C₃HMe₂)(μ -OH)Lu(CpC₂H₄)₂O] (Lu–O(OH) 2.154(3) Å).⁴² H₄Ba₆(μ_6 -O)(OC₂H₄OMe)₁₄ was reported as an oxo cluster where the hydrogen atoms could not be exactly located.⁴³ In this context and by considering the limited quality of the structural data, **3a** might be alternatively described as a “dioxo/alcohol” rather than an “oxo/hydroxo/alkoxide” cluster. However, IR spectroscopy (sharp ν (OH) vibration) and the intrinsic coordination of the core atoms (coordination number, symmetry behavior) favor the discussed “oxo/hydroxo/alkoxide” unit. For example, most lanthanide oxo clusters exhibit a central O²⁻ with coordination numbers of 4–6.^{31,32} Hydroxo ligands prefer the μ_3 -OH coordination mode as evidenced for “aqueous media” systems

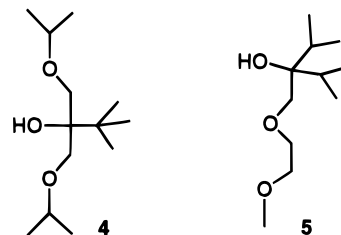


Figure 5. Potentially tridentate donor-functionalized alcohols.

Er₈(μ_4 -O)(thd)₁₀(OH)₂,^{4c} Ln₄(μ_3 -OH)₂(acac)₁₀ (Ln = Y, Nd),⁴⁴ and Ce₆(μ_3 -O)₄(μ_3 -OH)₄(acac)₁₂.⁴⁵

A preliminary investigation of the directed synthesis of **3a** verified by addition of a stoichiometric amount of water to alcohol **1a** prior to the alcoholysis reaction afforded a material whose elemental analysis ranges between that of **2a** and **3a**. The most striking similarity is the sharp IR absorption band of 3490 cm⁻¹ in the ν (OH) region. Apparently, the amount of water directs the yield of **3**.

Synthesis of Donor-Functionalized Alkoxides of Neodymium Bearing Tridentate Ligands. Reaction of Nd[N-(SiMe₃)₂]₃ with 3 equiv of tridentate donor-functionalized alcohols as depicted in Figure 5 was performed analogously to Scheme 2. The resulting light-blue complexes **6** and **7**, respectively, were characterized by IR spectroscopy, elemental analysis, and their sublimation behavior. CI mass spectrometry of **6** revealed the presence of dinuclear species in the gas phase. Similar findings have been made, when ligand **6** was employed for the synthesis of homoleptic donor-functionalized alkoxides of the alkaline earth metals.⁴⁶ The molecular structure of the complex {Ca[OCtBu(CH₂OiPr)₂]₂}₂ revealed that the ligand acts exclusively as a bidentate ligand.

Survey of the Sublimation Behavior of Donor-Functionalized Alkoxides of the Rare Earth Elements. Examination of the sublimation behavior of aliphatic, donor-functionalized alkoxides of the lanthanide elements reveals that mononuclearity is not a prerequisite or the utmost criterion for volatility (Table 3). All donor-functionalized alkoxides **2** presented in this work are most likely dinuclear in the solid state and still compare well with the monomeric congeners exhibiting a sterically demanding group in the α -position, e.g., Y(OCiPr₂CH₂OEt)₃ vs [Lu(OCMe₂CH₂OMe)₃] (**2a**). Examination of the crystal packaging of **2a** reveals no close intermolecular contacts. The significantly enhanced volatility of amino-functionalized alkoxides is probably due to the stronger donor capability of the amino group which might suppress the “arm on–arm off” process during heating. Furthermore, the bulkier donor moiety NMe₂ compared to OMe accomplishes both a sterically and electronically increased shielding of the strongly polarized Lu–O bond. As a consequence decreased intermolecular interactions result. Surprisingly, the “lutetium cluster” **3** is still volatile and sublimates at an elevated temperature comparable to Ln₅O(OiPr)₁₃.⁴⁷ The neodymium derivatives of the potentially tridentate alcohols **4** and **5** are less volatile. Although, these complexes appear to be dinuclear in the gas phase according to their mass spectra, enhanced volatility seems to be hampered by the higher mass

(37) Schumann, H.; Palamidis, E.; Loebel, J. *J. Organomet. Chem.* **1990**, *384*, C49.

(38) Daniele, S.; Hubert-Pfalzgraf, L. G.; Vaissermann, J. *Polyhedron* **1995**, *14*, 327.

(39) (a) Goodgame, D. M. L.; Williams, D. J.; Winpenny, R. E. P. *Polyhedron* **1989**, *8*, 1531. (b) Blake, A. J.; Milne, P. E. Y.; Thornton, P.; Winpenny, R. E. P. *Angew. Chem., Int. Ed. Engl.* **1991**, *30*, 1139.

(40) (a) Wang, S. *Inorg. Chem.* **1991**, *30*, 2252. (b) Wang, S.; Pang, Z.; Wagner, M. J. *Inorg. Chem.* **1992**, *31*, 5381. (c) Chen, X.-M.; Aubin, S. M. J.; Wu, Y.-L.; Yang, Y.-S.; Mak, T. C. W.; Hendrickson, D. N. *J. Am. Chem. Soc.* **1995**, *117*, 9600.

(41) Evans, W. J.; Sollberger, M. S.; Ziller, J. W. *J. Am. Chem. Soc.* **1993**, *115*, 4120.

(42) Schumann, H.; Loebel, J.; Pickardt, J.; Qian, C.; Xie, Z. *Organometallics* **1991**, *10*, 215.

(43) Caulton, K. G.; Chisholm, M. H.; Drake, S. R.; Huffman, J. C. *J. Chem. Soc., Chem. Commun.* **1990**, 1498.

(44) Poncelet, O.; Hubert-Pfalzgraf, L. G. *Polyhedron* **1989**, *8*, 2183.

(45) Toledano, P.; Ribot, F.; Sanchez, C. C. *R. Acad. Sci. Paris* **1990**, *311*, 1315.

(46) (a) Herrmann, W. A.; Huber, N. W. *Chem. Ber.* **1994**, *127*, 821. (b) Herrmann, W. A.; Huber, N. W.; Priermeier, T. *Angew. Chem., Int. Ed. Engl.* **1994**, *33*, 105.

(47) (a) Poncelet, O.; Sartain, W. J.; Hubert-Pfalzgraf, L. G.; Foltling, K.; Caulton, K. G. *Inorg. Chem.* **1989**, *28*, 263. (b) Helgesson, G.; Jagner, S.; Poncelet, O.; Hubert-Pfalzgraf, L. G. *Polyhedron* **1991**, *10*, 1559. (c) Bradley, D. C.; Chudzynska, H.; Hammond, M. E.; Hursthouse, M. B.; Motevalli, M.; Ruowen, W. *Polyhedron* **1992**, *11*, 375.

Table 3. Sublimation Behavior of Donor-Functionalized Alkoxides (Siloxides) of the Lanthanides

compd	sublimation temp (°C)	P (Torr)	ref
{Nd(OCH ₂ BuCH ₂ OEt) ₃ }	175	10 ⁻³	7
{Nd(OCH ₂ BuCH ₂ NEt ₂) ₃ }	150	10 ⁻³	7
Nd(OC ₂ Bu ₂ CH ₂ OEt) ₃	125	10 ⁻³	7
Nd(OC ₂ Pr ₂ CH ₂ OEt) ₃	115	10 ⁻³	7
Y(OC ₂ Pr ₂ CH ₂ OEt) ₃	95	10 ⁻³	7
[Lu(OCMe ₂ CH ₂ OMe) ₂] (2a)	95	10 ⁻³	7
{Y(OCEt ₂ CH ₂ OMe) ₃ } (2b)	160	10 ⁻³	a
{Lu(OCMe ₂ CH ₂ NMe ₂) ₃ } (2c)	75	10 ⁻³	a
{Y(OCMe ₂ CH ₂ NMe ₂) ₃ } (2d)	80	10 ⁻³	a
Lu ₄ (O)(OH)(OCMe ₂ CH ₂ OMe) ₉ (3)	>220	10 ⁻³	a
{Nd[OC ₂ Bu(CH ₂ OiPr) ₂] ₃ } (6)	140	10 ⁻³	a
{Nd(OC ₂ Pr ₂ CH ₂ OCH ₂ CH ₂ OMe) ₃ } (7)	140	10 ⁻³	a
Y[OSi ₂ Bu ₂ (CH ₂) ₃ NMe ₂] ₃	115	5 × 10 ⁻⁴	14a
Ce[OSi ₂ Bu ₂ (CH ₂) ₃ NMe ₂] ₃	135	5 × 10 ⁻⁴	14a
Y[OSi ₂ Bu ₂ (CH ₂) ₃ NMe ₂] ₃ [OSi ₂ Bu ₂ (CH ₂) ₃ NMe ₂ H]	125	5 × 10 ⁻⁴	14a

^a This work.

of the ligands. The presence of an increased number of dangling donor functionalities, which markedly disturbs the spherical shape of the molecule, further counteracts the volatility of **6** and **7**.⁴⁸

Conclusion

The results presented here are part of our program “design and evaluation of donor-functionalized alkoxides as molecular precursors to ceramic materials”. Initial attempts to isolate mononuclear lanthanide derivatives of type [Ln(OCR₂CH₂do)₃] revealed the importance of having sterically bulky groups in the α-position to the O(alkoxide) atom. Now, further variation of the ligand sphere allows a more general interpretation of this type of alkoxide ligands. The reduction of steric bulk R in the α-position leads, as expected, to higher agglomerated systems as evidenced for homoleptic, dinuclear **2a** which reveals intriguing structural features. The enhanced steric flexibility of OCMe₂CH₂OMe is expressed in at least six different coordination modes: μ₃,η²-OR (asym); μ₂,η²-OR (sym, asym); μ₂,η¹-OR (sym); η²-OR; η¹-OR. **2a** comprises a rather unusual asymmetrically triple-bridging structural motif rendering metal centers coordinated by four and five alkoxide ligands, respectively. The formation of the unprecedented oxo hydroxo lutetium alkoxide **3a** could be traced back to the presence of water and, once more, shows that incorporation of oxo and hydroxo ligands into lanthanide alkoxides counteracts the denucleation properties of multidentate alkoxide ligands. In contrast, formation of the most popular lanthanide alkoxide cluster, Ln₅O(OiPr)₁₃, was explained by deoxygenation of the alcohol and elimination of diisopropyl ether as a consequence of the strong oxophilic behavior of the lanthanides rather than by “hydrolysis by chance”.⁴⁷

The sublimation behavior of the dinuclear complexes **2** show that increased molecular weight does not necessarily result in decreased volatility but emphasizes that volatility is predominantly controlled by molecular (ligand) shape and crystal packing. The complexes reported here belong to the most volatile rare earth complexes. The exciting molecular structure of **2a** stimulates a more detailed investigation of such donor-functionalized alkoxides. We are currently examining the impact of steric bulk in β-position and variation of the donor functionalities according to the hard/soft principle on the habit of donor-functionalized alkoxides. In addition, studies concern-

ing the role of water in the degradation process of donor-functionalized alkoxy derivatives of the lanthanides are in progress.

Experimental Section

General Remarks. All manipulations of air-sensitive materials were performed under argon using standard Schlenk, high-vacuum, and glovebox techniques (<2 ppm O₂, <1 ppm H₂O). Solvents were distilled from Na/K alloy under argon. LiNMe₂ (Aldrich) and 2-methyl-1-propenoxide (Lancaster) were used as received. Donor-functionalized alcohols **1a**, **1b**, **4**, and **5** were prepared as previously described and dried over molecular sieves (3 Å) prior to use.^{16,46} Anhydrous NdCl₃, YCl₃ (Johnson Matthey), and LuCl₃ (Strem) were used as purchased. Ln[N(SiMe₃)₂]₃ were synthesized according to ref 49 and sublimed before use.

The organic syntheses were assisted by gas chromatographic analyses using a Beckman HP5890 instrument with HP5970 mass filter. Infrared spectra were recorded as Nujol mulls between CsI plates (metal complexes) or fluid films (organic compounds) on a Perkin Elmer 1600 series FT-IR spectrometer. NMR spectra were performed on a JEOL-JMN-GX 400 instrument (400 MHz, ¹H; 100.54 MHz, ¹³C). All spectra were recorded at ambient temperature unless otherwise noted. Mass spectra were obtained on a Varian-MAT 311A spectrometer (EI method) and a Varian-MAT 90 spectrometer (CI, FI method). Elemental analyses were performed by the microanalytical laboratory in Munich.

HOCMe₂CH₂NMe₂ (1c). A solution of 2-methyl-1-propenoxide (7.21 g, 100 mmol) in THF (20 mL) was slowly added to a stirred and precooled (0 °C) solution of LiNMe₂ (5.11 g, 100 mmol) in THF (50 mL). The mixture was stirred overnight at ambient temperature and then quenched with a stoichiometric amount of water (1.80 g, 100 mmol). The resulting THF portion was dried over magnesium sulfate, and product **1c** was obtained by fractional distillation in 53% yield (6.21 g). **1c** was postdried over molecular sieves (3 Å). Bp: 121 °C. MS (EI): *m/z* 117 (4) [M⁺], 102 (10) [M⁺ - Me], 58 (100) [CH₂-NMe₂⁺]. ¹H NMR (C₆D₆): δ 1.12 (s, 6 H, CCH₃), 2.04 (s, 2 H, CH₂), 2.12 (s, 6 H, NCH₃), 2.95 (s, 1 H, OH). ¹³C{¹H} NMR (C₆D₆): δ 28.3 (CCH₃), 48.2 (NCH₃), 69.8 (CCH₃), 70.2 (CH₂). Anal. Calcd for C₆H₁₅NO (117.2): C, 61.49; H, 12.90; N, 11.95. Found: C, 61.03; H, 13.09; N, 11.55.

Synthesis of Donor-Functionalized Alkoxides. The preparation of alkoxide complexes **2**, **6**, and **7** was identical and is described in detail for **2a**.

Lu(OCMe₂CH₂OMe)₃ (2a). In a glovebox, **1a** (0.324 g, 3.11 mmol) dissolved in 15 mL of *n*-hexane was added dropwise to a stirred solution of Lu[N(SiMe₃)₂]₃ (0.680 g, 1.04 mmol) in 35 mL of *n*-hexane. The resulting clear solution was stirred overnight at ambient temperature. Evaporation of the solvent and the produced silylamine, followed by drying under high vacuum (10⁻³ Torr) for 5 h, gave **2a** as white

(48) Anwander, R.; Herrmann, W. A.; Scherer, W.; Munck, F. C. J. *Organomet. Chem.* **1993**, *462*, 163.

(49) Herrmann, W. A.; Anwander, R.; Kleine, M.; Scherer, W. *Chem. Ber.* **1992**, *125*, 1971.

microcrystalline powder in quantitative yield (0.499 g). IR: 1366 (sh) vs, 1348 s, 1279 s, 1266 (sh) m, 1227 s, 1212 (sh) s, 1178 vs, 1155 (sh) s, 1108 s, 1076 vs, 1064 (sh) s, 1027 s, 1098 s, 996 s, 980 vs, 959 vs, 934 m, 910 (sh) m, 895 w, 847 w, 823 w, 796 m, 777 w, 737 (sh) w, 723 w, 668 w, 576 s, 506 (sh) w, 496 (sh) m, 487 m, 477 m, 434 w, 416 w cm^{-1} . MS (CI): m/z 865 (100) [$2\text{M}^+ - \text{OR}$], 851 (4) [$2\text{M}^+ - \text{OR} - \text{M} + 1$], 381 (2) [$\text{M}^+ - \text{OR}$]. ^1H NMR (C_6D_6): δ 1.44 (s, 6H, CCH_3), 3.32 (s, 2H, CH_2), 3.46 (s, 3H, OCH_3). $^{13}\text{C}\{^1\text{H}\}$ NMR (C_6D_6): δ 29.6 (CCH_3), 59.6 (OCH_3), 70.7 (OCH_2), 85.9 (CCH_3). Anal. Calcd for $\text{C}_{15}\text{H}_{33}\text{O}_6\text{Lu}$ (484.4): C, 37.19; H, 6.87. Found: C, 37.23; H, 6.91.

Y(OCe₂CH₂OMe)₃ (2b). Addition of a solution of **1b** (0.541 g, 3.89 mmol, 10 mL of *n*-hexane) to a stirred solution of $\text{Y}[\text{N}(\text{SiMe}_3)_2]_3$ (0.741 g, 1.3 mmol, 25 mL of *n*-hexane) and subsequent workup afforded **2b** as a white solid in quantitative yield (0.615 g). IR: 1337 w, 1325 w, 1293 w, 1265 w, 1216 (sh) w, 1202 (sh) w, 1192 m, 1167 s, 1150 s, 1110 s, 1085 vs, 1065 m, 1049 m, 1038 m, 1001 s, 989 s, 930 s, 906 m, 804 w, 770 w, 739 w, 723 w, 668 w, 606 w, 586 w, 533 w, 494 w, 481 w, 465 w, 438 w, 418 w cm^{-1} . MS (CI): m/z 600 (100) [$2\text{M}^+ - 2\text{OR} - \text{CH}_2\text{OMe} + \text{H}$], 483 (3) [$\text{M}^+ + \text{H}$], 115 (41) [$\text{OR}^+ - \text{Me} - \text{H}$], 103 (2) [$\text{HOR}^+ - \text{Et}$]. Anal. Calcd for $\text{C}_{21}\text{H}_{45}\text{O}_6\text{Y}$ (482.5): C, 52.28; H, 9.40. Found: C, 52.14; H, 9.54.

Lu(OCMe₂CH₂NMe₂)₃ (2c). Addition of a solution of **1c** (0.228 g, 1.95 mmol, 15 mL of *n*-hexane) to a stirred solution of $\text{Lu}[\text{N}(\text{SiMe}_3)_2]_3$ (0.426 g, 0.65 mmol, in 35 mL of *n*-hexane) and subsequent workup afforded **2c** as an oily residue in quantitative yield (0.336 g). IR: 2764 s, 1365 (sh) s, 1348 m, 1302 m, 1265 m, 1209 s, 1175 s, 1150 vs, 1131 s, 1041 s, 1012 vs, 979 m, 952 s, 946 s, 910 w, 863 w, 841 w, 797 m, 723 w, 602 w, 592 w, 581 w, 511 w, 499 w, 471 w, 431 w cm^{-1} . MS (CI): m/z 930 (6) [$2\text{M}^+ - \text{OR}$], 118 (100) [$\text{HOR}^+ + \text{H}$]. ^1H NMR (C_6D_6): δ 1.52 (s, 6H, CCH_3), 2.41 (s, 6H, NCH_3), 2.44 (s, 2H, CH_2). $^{13}\text{C}\{^1\text{H}\}$ NMR (C_6D_6): δ 33.1 (CCH_3), 48.2 (NCH_3), 73.0–75.3 (br, CH_2 , CCH_3). Anal. Calcd for $\text{C}_{18}\text{H}_{42}\text{O}_3\text{N}_3\text{Lu}$ (523.52): C, 41.30; H, 8.09; N, 8.03. Found: C, 41.40; H, 8.41; N, 7.82.

Y(OCMe₂CH₂NMe₂)₃ (2d). Addition of a solution of **1c** (0.307 g, 2.62 mmol, 15 mL of *n*-hexane) to a stirred solution of $\text{Y}[\text{N}(\text{SiMe}_3)_2]_3$ (0.467 g, 0.87 mmol, 35 mL of *n*-hexane) and subsequent workup afforded **2d** as an oily residue in quantitative yield (0.376 g). IR: 2764 s, 1365 (sh) s, 1347 s, 1301 m, 1264 m, 1208 s, 1173 s, 1149 vs, 1130 s, 1096 w, 1041 vs, 1007 vs, 981 m, 951 s, 908 m, 862 w, 839 w, 796 m, 766 w, 723 w, 590 m, 579 m, 508 w, 488 w, 473 w, 430 m cm^{-1} . MS (CI): m/z 758 (100) [$2\text{M}^+ - \text{OR}$], 700 (3) [$2\text{M}^+ - \text{OR} - \text{CH}_2\text{NMe}_2$]. ^1H NMR (C_6D_6): δ 1.51 (s, 6H, CCH_3), 2.41 (s, 6H, NCH_3), 2.49 (s, 2H, CH_2). ^{13}C NMR (C_6D_6): δ 33.1 (q, $^1J(\text{C},\text{H}) = 124$ Hz, CCH_3), 48.3 (q, $^1J(\text{C},\text{H}) = 128$ Hz, NCH_3), 72.8 (s, CCH_3), 74.2 (t, $^1J(\text{C},\text{H}) = 131$ Hz, CH_2). Anal. Calcd for $\text{C}_{18}\text{H}_{42}\text{O}_3\text{N}_3\text{Y}$ (437.23): C, 49.40; H, 9.68; N, 9.61. Found: C, 49.32; H, 9.66; N, 9.36.

Lu₄(O)(OH)(OCMe₂CH₂OMe)₉ (3a). In a glovebox, 0.51 g (0.78 mmol) of $\text{Lu}[\text{N}(\text{SiMe}_3)_2]_3$ was suspended in 25 mL of *n*-hexane. The suspension was cooled to -35 °C and then treated with alcohol **1a** (0.24 g, 2.30 mmol; not predried over molecular sieves) by slow addition. The resulting cloudy solution (slightly white precipitate) was stirred for 88 h at room temperature. After filtration, the filtrate was evaporated to dryness. The thus obtained residue was further dried under high vacuum (10^{-3} Torr) for 6 h to give a white powder, designated as **3** (0.30 g). **3** can be sublimed above 220 °C/ 10^{-3} Torr. Crystallization of the sublimed material from *n*-hexane yielded a few single crystals (**3a**). IR (**3**): $\nu = 3487$ m, 1364 s, 1348 m, 1285 m, 1276 m, 1236 m, 1204 m, 1180 vs, 1157 (sh) m, 1102 s, 1078 s, 1070 m, 1061 m, 1018 s, 985 s, 970 vs, 954 m, 941 (sh) m, 920 w, 902 w, 796 w, 778 w, 669 w, 636 m, 577 m, 523 w, 494 w, 476 w, 453 w, 434 w cm^{-1} . MS (CI, **3**), m/z (%) = 1557 (4) [$\text{Lu}_3(\text{OR})_9(\text{HOR})^+$], 1452 (6) [$\text{Lu}_3(\text{OR})_9^+$], 991 (69), 961 (23), 865 (100) [$\text{Lu}_2(\text{OR})_5^+$]. Anal. Calcd for $\text{C}_{45}\text{H}_{100}\text{Lu}_4\text{O}_{20}$ (**3a**, 1661.15): C, 32.54; H, 6.07. Found: C, 30.43; H, 5.84 (**3a**); C, 31.13; H, 5.04 (sublimed **3**).

Nd[OC*t*Bu(CH₂O*i*Pr)₂]₃ (6). Addition of a solution of **4** (0.920 g, 3.96 mmol, 10 mL of *n*-hexane) to a stirred solution of $\text{Nd}[\text{N}(\text{SiMe}_3)_2]_3$ (0.813 g, 1.30 mmol, 45 mL of *n*-hexane) and subsequent workup afforded **6** as a light blue solid in quantitative yield (1.078 g). IR: 1365 (sh) m, 1335 m, 1295 m, 1257 w, 1233 w, 1159 vs, 1143 (sh) vs, 1126 vs, 1097 vs, 1066 vs, 1040 s, 1009 m, 998 m, 968 s, 936 m, 896

Table 4. Crystallographic Data for $\text{Lu}_2(\mu_2, \eta^2\text{-OR})_3(\eta^2\text{-OR})(\eta^1\text{-OR})_2$ (**2a**) and $\text{Lu}_4(\mu_4\text{-O})(\mu_3\text{-OH})(\mu_3, \eta^2\text{-OR})(\mu_2, \eta^2\text{-OR})_3(\mu_2, \eta^1\text{-OR})(\eta^1\text{-OR})_4$ (**3a**)

formula	$\text{C}_{30}\text{H}_{66}\text{Lu}_2\text{O}_{12}$	$\text{C}_{45}\text{H}_{100}\text{O}_{20}\text{Lu}_4$
fw	968.8	1661.1
space group	$P2_1/n$ (IT No. 14) ^c	Cc (IT No. 9)
<i>a</i> , Å	13.510(1)	21.63(1)
<i>b</i> , Å	15.130(1)	14.49(3)
<i>c</i> , Å	38.953(4)	21.04(2)
β , deg	93.11(1)	109.70(3)
<i>V</i> , Å ³	7950	6209
<i>Z</i>	8	4
<i>T</i> , K	213	163
λ , Å	Mo K α , 0.710 73	Mo K α , 0.710 73
ρ_{calcd} , g cm^{-3}	1.62	1.78
μ , mm^{-1}	4.95	6.4
no. of obsd rflns	11 747 ($I > 2.0\sigma(I)$)	6057 ($I > 3.0\sigma(I)$)
$R(F_o)^a$	3.5	6.7
$R_w(F_o)^b$	3.6	7.5

$$^a R = \sum |F_o| - |F_c| / \sum |F_o|. \quad ^b R_w = [\sum w(|F_o| - |F_c|)^2 / \sum w|F_o|^2]^{1/2}.$$

m, 841 w, 825 w, 811 w, 771 w, 729 w, 684 w, 612 m, 581 w, 566 w, 546 w, 513 w, 476 w, 459 w, 417 m cm^{-1} . MS (CI): m/z 1115 (3) [$2\text{M}^+ - 2\text{OR} - \text{iBu} - \text{iPr} + \text{H}$], 862 (100) [$2\text{M}^+ - 3\text{OR} - \text{CH}_2\text{O*i*Pr} - \text{iPr} - 2\text{H}$], 688 (7) [$\text{M}^+ - \text{CH}_2\text{O*i*Pr} - \text{iPr} - 2\text{H}$], 606 (41) [$\text{M}^+ - \text{OR}$], 233 (96) [$\text{HOR}^+ + \text{H}$]. Anal. Calcd for $\text{C}_{39}\text{H}_{81}\text{O}_9\text{Nd}$ (838.30): C, 55.88; H, 9.74. Found: C, 56.85; H, 9.56.

Nd(OC*i*Pr₂CH₂OCH₂CH₂OMe)₃ (7). Addition of a solution of **5** (0.844 g, 4.13 mmol, 25 mL of *n*-hexane) to a stirred solution of $\text{Nd}[\text{N}(\text{SiMe}_3)_2]_3$ (0.820 g, 1.31 mmol, 40 mL of *n*-hexane) and subsequent workup afforded **7** as a light blue solid in quantitative yield (0.978 g). IR: 1361 (sh) s, 1334 m, 1314 m, 1296 m, 1272 m, 1249 m, 1200 s, 1179 s, 1160 vs, 1113 vs, 1107 vs, 1099 vs, 1027 vs, 957 s, 934 s, 899 s, 842 s, 826 (sh) m, 745 w, 715 m, 677 m, 647 w, 634 w, 601 w, 576 w, 516 m, 472 w, 425 m cm^{-1} . MS (CI): m/z 954 (1) [$2\text{M}^+ - \text{Nd}(\text{OR})_2$], 923 (8) [$2\text{M}^+ - \text{Nd}(\text{OR})_2 - \text{OMe}$], 737 (1) [$\text{M}^+ - \text{Me} + \text{H}$], 665 (2) [$\text{M}^+ - 2\text{iPr}$], 662 (2) [$\text{M}^+ - \text{CH}_2\text{OCH}_2\text{CH}_2\text{OMe}$], 650 (1) [$\text{M}^+ - 2\text{iPr} - \text{Me}$], 549 (99) [$\text{M}^+ - \text{OR} + \text{H}$], 506 (2) [$\text{M}^+ - \text{OR} - \text{iPr} + \text{H}$], 188 (2) [$\text{OR}^+ - \text{Me}$], 161 (2) [$\text{HOR}^+ - \text{iPr}$], 115 (1) [$\text{HOR}^+ - \text{CH}_2\text{OCH}_2\text{CH}_2\text{OMe}$]. Anal. Calcd for $\text{C}_{33}\text{H}_{69}\text{O}_9\text{Nd}$ (754.14): C, 52.56; H, 9.22. Found: C, 53.94; H, 9.66.

X-ray Structure Determination of 2a. Crystals of compound **2a** were grown by slow evaporation of an *n*-hexane solution at ambient temperature. X-ray data were collected on a STOE Imaging Plate Detector System with a rotating anode X-ray generator (Enraf Nonius). The φ movement mode was oscillation. Final cell constants were obtained by least-squares refinement of 1942 reflections with $I/\sigma(I) > 50$ ($0^\circ < \varphi < 360^\circ$, $3.1^\circ < 2\theta < 50.2^\circ$) with the program CELL.⁵⁰ Details of data collection and refinement are presented in Table 4. Due to the very long crystallographic *c*-axis the data collection was done in two steps with different detector distances: one “inner” data set at 120 mm and one “outer” data set at 75 mm. The mean intensity of a maximum 20 (50) reflections ($I > 20$ (50) $\sigma(I)$) per image was monitored over the duration of the measurement for the two data sets. A slight decrease in intensity due to decomposition combined with variations due to absorption effects was corrected with the program “DECAY”⁵⁰ (smooth factor: 3). Both data sets were individually corrected for polarization effects and anomalous dispersion but not merged. Scaling, combining of the two data sets, sorting, and merging was done with the program CRYSTALS.⁵¹

A total of 130 852 reflections ($1.9^\circ < 2\theta < 50.2^\circ$) were collected in 80 h, 123 120 reflections of which with $I > 0$ were merged to give 13 860 independent reflections. A total of 11 747 reflections with $I/\sigma(I) > 2.0$ were used in the full-matrix refinement of 793 parameters. The structure was solved by direct methods⁵² followed by subsequent

(50) *IPDS Control Software*; STOE: Darmstadt, Germany, 1994.

(51) Watkin, D. J.; Betteridge, P. W.; Carruthers, J. R. *CRYSTALS User Manual*, Oxford University Computing Laboratory: Oxford, U.K., 1986.

(52) Altomare, A.; Casciarano, G.; Giacovazzo, C.; Guagliardi, A.; Burla, M. C.; Polidori, G.; Camalli, M. *SIR-92*; University of Bari: Bari, Italy, 1992.

difference Fourier techniques. All non-hydrogen atoms were refined freely with individual anisotropic thermal parameters, and all 132 hydrogen atoms were placed in calculated positions ($d_{C-H} = 96$ pm) and refined as "riding groups" together with their parent carbon atoms. The structure refinement converged at shift/error < 0.0003 , residual electron density $+0.91 \Delta e \text{ \AA}^{-3}$ (134 pm besides Lu(4)) and $-1.35 \Delta e \text{ \AA}^{-3}$. All calculations were performed on a DECstation 5000/25 using the programs CRYSTALS⁵¹ and PLATON.^{53a}

X-ray Crystallography of 3a. Compound **3a** crystallizes from a saturated *n*-hexane solution at -35 °C as colorless cubes. Preliminary examination and data collection were carried out with Mo K α radiation ($\lambda = 71.07$ pm; graphite monochromator) on an Enraf-Nonius CAD4 diffractometer at -110 ± 3 °C. Details of data collection and refinement are presented in Table 4. Data were collected in the ω -scan mode, orientation control reflections were monitored every 200th reflection, and the intensities of three reflections were checked every 3600 s. Changes in intensities were corrected. An absorption correction based on Ψ -scan data was done. Structure determination was with Patterson methods and subsequent difference Fourier maps. Full-matrix least-squares refinement was carried out by minimizing $\sum w(|F_o| - |F_c|)^2$ (unit weights). Hydrogen atoms were calculated in their ideal positions, included in the data set but not refined. Scattering factors and

anomalous dispersion corrections were taken from ref 54. The refinement stopped at shift/err < 0.001 , and final difference Fourier maps showed no significant features. The refinement of the enantiomorphic structure model resulted in higher *R*-values ($R = 0.072$; $R_w = 0.079$). All calculations were performed on a DECstation 5000/25 using the programs CRYSTALS,⁵¹ SDP,⁵⁵ and PLATON.^{53a}

Acknowledgment. We thank the OSRAM GmbH for generous support for this research and the Deutsche Forschungsgemeinschaft for a fellowship (to R.A.). We are grateful to Dr. N. W. Huber for support of alcohols **1b,d,e** and Dr. Peter Härter for assistance during the NMR measurements. M. Barth and his co-workers are acknowledged for performing the elemental analyses, and apl. Prof. F. R. Kreissl and R. Dumitrescu, for recording the mass spectra.

Supporting Information Available: X-ray crystallographic files, in CIF format, for compounds **2a** and **3a** are available on the Internet only. Access information is given on any current masthead page.

IC9700157

(53) (a) Spek, A. L. The "Euclid" package. In *Computational Crystallography* Sayre, D., Ed.; Clarendon Press: Oxford, U.K., 1982. (b) Keller, E. *SCHAKAL, Ein Programm für die graphische Darstellung von Molekülmodellen*; Kristallographisches Institut, Universität Freiburg: Freiburg, Germany, 1986/1988.

(54) (a) Cromer, D. T. *International Tables of Crystallography*; Kynoch Press: Birmingham/England, 1974. (b) Sheldrick, G. M. *Shelx-86*; Universität Göttingen: Göttingen, Germany, 1986.

(55) Frenz, B. A. The ENRAF-NONIUS CAD4 SDP SYSTEM. In *Computing in Crystallography*; Delft University Press: Delft, Holland, 1978.